frontiers | Frontiers in Chemical Engineering

ORIGINAL RESEARCH
published: 26 April 2022
doi: 10.3389/fceng.2022.877255

Polyaniline on Stainless Steel Fiber Felt as Anodes for Bioelectrodegradation of Acid Blue 29 in Microbial Fuel Cells

Mohammad Danish Khan[1,2], *Shamas Tabraiz*[2,3], *Ravikumar Thimmappa*[2], *Da Li*[4], *Abdul Hakeem Anwer*[1], *Keith Scott*[2], *Mohammad Zain Khan*[1]* and *Eileen Hao Yu*[4]*

[1]Industrial Chemistry Research Laboratory, Department of Chemistry, Aligarh Muslim University, Aligarh, India, [2]School of Engineering, Newcastle University, Newcastle upon Tyne, United Kingdom, [3]School of Natural and Applied Sciences, Canterbury Christ Church University, Canterbury, United Kingdom, [4]Department of Chemical Engineering, Loughborough University, Loughborough, United Kingdom

This study investigated the advantages of using low-cost polyaniline-fabricated stainless steel fiber felt anode-based microbial fuel cells (PANI-SSFF-MFCs) for azo dye acid blue 29 (AB29) containing wastewater treatment integrated with an aerobic bioreactor. The findings of electrochemical impedance spectroscopy (EIS) and polarization studies showed that the PANI–SSFF anode considerably decreased the MFC internal resistance. The highest power density of 103 ± 3.6 mW m^{-2} was achieved by PANI-SSFF-MFCs with a decolorization efficiency of 93 ± 3.1% and a start-up time of 13 days. The final chemical oxygen demand (COD) removal efficiencies for integrated PANI–SSFF–MFC–bioreactor and SSFF–MFC–bioreactor set-ups were 92.5 ± 2% and 80 ± 2%, respectively. Based on 16S rRNA gene sequencing, a substantial microbial community change was observed in MFCs. The majority of sequences were from the *Proteobacteria* phylum, accounting for 72% and 55% in PANI–SSFF–anodic biofilm and suspension, respectively, and 58 and 45% in SSFF–anodic biofilm and suspension, respectively. The relative abundance of the seven most abundant genera (*Pseudomonas, Acinetobacter*, *Stenotrophomonas, Geothrix*, *Dysgonomonas, Shinella*, and *Rhizobiales*) was higher in PANI–SSFF–MFCs (46.1% in biofilm and 55.4% in suspension) as compared to SSFF–MFC (43% in biofilm and 40.8% in suspension) which predominantly contributed to the decolorization of AB29 and/or electron transfer. We demonstrate in this work that microbial consortia acclimated to the MFC environment and PANI-fabricated anodes are capable of high decolorization rates with enhanced electricity production. A combined single-chamber MFC (SMFC)-aerobic bioreactor operation was also performed in this study for the efficient biodegradation of AB29.

Keywords: microbial fuel cells, stainless steel fiber felt, polyaniline, acid blue 29 biodegradation, power generation, microbial community

OPEN ACCESS

Edited by:
Costas Tsouris,
Oak Ridge National Laboratory (DOE), United States

Reviewed by:
MaurÃ-cio Alves Motta Sobrinho, Federal University of Pernambuco, Brazil
Aikaterini Ioannis Vavouraki, Technical University of Crete, Greece

***Correspondence:**
Mohammad Zain Khan
dr_mzain.fa@amu.ac.in
Eileen Hao Yu
e.yu@lboro.ac.uk

Specialty section:
This article was submitted to Sustainable Process Engineering, a section of the journal Frontiers in Chemical Engineering

Received: *16 February 2022*
Accepted: *28 March 2022*
Published: *26 April 2022*

Citation:
Khan MD, Tabraiz S, Thimmappa R, Li D, Anwer AH, Scott K, Khan MZ and Yu EH (2022) Polyaniline on Stainless Steel Fiber Felt as Anodes for Bioelectrodegradation of Acid Blue 29 in Microbial Fuel Cells. Front. Chem. Eng. 4:877255. doi: 10.3389/fceng.2022.877255

Abbreviations: AB29, acid blue 29; CE, Coulombic efficiency; CEM, cation exchange membrane; COD, chemical oxygen demand; CPD, critical point dryer; CV, cyclic voltammetry; EAB, electrochemically active Bacteria; EIS, electrochemical impedance spectroscopy; FePc, iron Phthalocyanine; GC, gas chromatography; GCD, galvanostatic charge-discharge; GDL, gas diffusion layer; MS, mass spectrometry; NMDS, non-metric multidimensional scaling; PANI, polyaniline; RE, removal efficiencies; SEM, scanning electron microscopy; SMFC, single-chamber microbial fuel cells; SSFF, stainless steel fiber felt.

INTRODUCTION

Azo dyes are widely used in several industries, including textiles, leather, plastics, food, printing, and cosmetics, representing over 70% of industrial dye usage worldwide (Rawat et al., 2016). Discharging azo dye-laden colored wastewater into water bodies is objectionable. Moreover, various azo dyes and their degraded chemical intermediates are deleterious to human and animal health, aquatic life, and the environment (Khan et al., 2015a; Khan et al., 2015b). It is challenging to degrade azo dyes due to their complex aromatic structures having azo bonds (–N=N–) of high-bond energy. Many physical and chemical treatment approaches such as adsorption, ion exchange, membrane separation, advanced oxidation, ozone treatment, photocatalytic, and coagulation-flocculation have been established to decolorize or degrade these azo dye-containing wastewater; however, they use a significant amount of chemicals and the operating cost is too high (Solanki et al., 2013). Conventional biological anaerobic degradation approaches have also been investigated for azo dye-laden wastewater treatment; however, they create a high quantity of sludge that requires safe and secure dumping (Yang et al., 2019). Aerobic biodegradation of azo dyes is challenging; however, decolorization of azo dyes can be accomplished in an anaerobic environment, while the colorless aromatic amine can be easily treated aerobically (Khan MD. et al., 2015; Sultana et al., 2015). Therefore, an integration of anaerobic and aerobic methods has been progressively studied to treat azo dye-laden wastewater (Fernando et al., 2014; Popli and Patel, 2015; Khan N et al., 2021). The microbial fuel cell (MFC) is an innovative technology that can speed up the process of decolorization. An MFC combines the benefits of traditional biological and electrochemical processes. The expeditious advancement of research on MFC as a treatment technology has prompted plenty of content in portraying this technology and the fundamental process. Various mono and diazo dyes have been reported to be decolorized in MFCs (Solanki et al., 2013).

On the other side, MFCs suffer problems, for example, low power production and expensive electrode material, especially with the utilization of comparatively costly anode materials, limiting their extensive use and commercialization (Khan et al., 2017). The anode materials perform a significant role in bioelectricity production by an MFC by providing the actual available surface area for a wide coverage of exoelectrogenic bacteria and affecting the interfacial electron transfer resistance (Mehdinia et al., 2013). Consequently, it is extremely necessary to choose the anodic materials which have low-charge transfer resistance and overpotential, are biocompatible, chemically stable, and resist corrosion. It has been previously reported that stainless steel (SS) can be used as an anode material that is effective and promising in MFCs (Paquin et al., 2015). However, SS has some intrinsic properties that restrict its use as anodes for large-scale bioelectricity generation, such as poor biocompatibility compared to that of carbon-based anodes, and due to this drawback, electroactive biofilm forms on the surface is poor (Sonawane et al., 2018a). It has been recommended that by fabricating SS with polyaniline (PANI), these properties of SS can be enhanced (Hou et al., 2015). PANI can be coated on electrodes either by electrochemical oxidative polymerization or chemical oxidation of aniline. PANI has been generally utilized for modifying electrodes in MFC and showed that it could effectively improve the performance of MFC. PANI modification can improve MFC performance by increasing microbial adhesion and play a significant role as biocatalysts (Lai et al., 2011; Hou et al., 2015; Sonawane et al., 2018a). Moreover, the cathode materials are equally significant and substantially impact MFC efficiency and performance. Carbon-supported iron phthalocyanine (FePc/C) has the capability to encourage direct $4e^-$ oxygen reduction (de Oliveira et al., 2020).

Several works have been reported with toxic azo dyes being treated in the anodic chamber of MFC with PANI-modified anodes. An earlier work carried out by Zhong et al. (2018) has reported the use of PANI-modified carbon felt anode in microbial fuel cell MFC, which was found to be highly efficient in terms of color removal (96%) and COD removal (64%) efficiencies of Reactive Brilliant Red X-3B (50 mg L-1) reached at 48 h. In other work, the efficient decolorization of the azo dye, Congo red, containing wastewater with PANI-based anode in microbial electrochemical systems. The dye decolorization reached 90% at 54 h (Li et al., 2022). Dessie et al. (2022) reported methyl red decolorization efficiency of 95.57% by a MnO_2/PANI anode in a dial chamber MFC. Moreover, research works published by Hou et al. (2015) further verified the high efficiency of PANI-coated SSFF. They reported a maximum cell potential of 550 mV within 14 days using acetate as a carbon source. These studies presented the effect of the PANI-coated electrode on the performance of MFC treating wastewater.

In this study, we used PANI to modify the stainless steel fibre felt (SSFF) anode in order to boost MFC performance. PANI was coated on SSFF by galvanostatic electropolymerization. The FePc/C catalyst has been prepared and coated on air cathodes and extended for the feasibility studies in MFCs treating azo dye-laden wastewater. To the authors knowledge, there is not any study in detail on the usage of PANI modified SSFF anode and FePc/C modified cathode for MFCs treating azo dye acid blue 29 (AB29). Therefore, this research work aimed to get a deeper understanding of the properties and nature of fabricated electrodes, as well as their impact on MFC performance. The AB29 was selected as a diazo dye in this work, and the decolorization percentage, bioelectricity generation, and chemical oxygen demand (COD) removal percentage were evaluated. Moreover, the microbial community analysis of biofilm and suspension of MFCs was also done to reveal the dominance of dye degrading bacteria and electrogens in MFCs. Understanding azo dye degradation in combined MFCs and anaerobic processes will enable further optimization of the process to treat azo dye-laden wastewater and power generation simultaneously.

MATERIALS AND METHODS

Chemicals and Materials

Xi'an Filter Metals Materials Co., Ltd (China), supplied the anode material SSFF (BZ40D, thickness 0.4 mm), having a porosity of

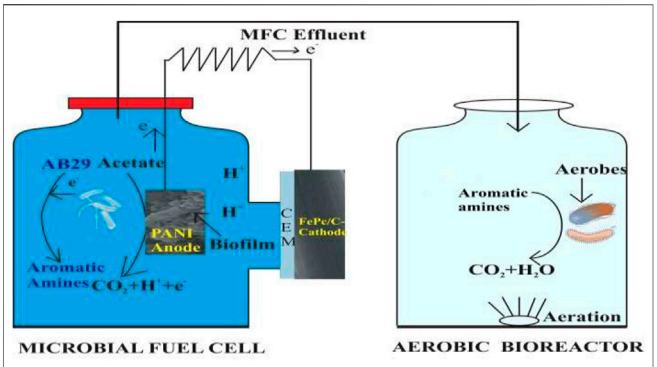

FIGURE 1 | Integrated SMFC–aerobic bioreactor set-up.

78 ± 5% and pore size of 28.9 µm. Quintech (H2315 I2 C6, Germany) provided carbon paper having a gas diffusion layer (GDL). GDL was purchased from Quintech (H2315 I2 C6, Germany). Unless specified otherwise, all chemicals used in this work were analytically graded (Sigma Aldrich, United Kingdom).

Preparation of Catalyst and Electrode

The SSFFs were cut into 3 cm × 3 cm pieces and sonicated in acetone and ethanol for 15 min each to eliminate any remaining organic matter before being rinsed with distilled water and dried. The electropolymerization of aniline was conducted by galvanostatic polymerization in 0.5 M H_2SO_4 acidic solution containing 0.1 M aniline in a three-electrode mode with an AutoLab potentiostat (PGSTAT204, Metrohm, Netherlands). Before beginning polymerization, a 15 min N_2 gas purge was performed to eliminate oxygen from the solution. The SSFF was working, a Pt mesh was a counter electrode, and Ag/AgCl (+0.205 V vs. SHE) functioned as a reference electrode. PANI coating on the SSFF was achieved using a current density of 2.5 mA cm^{-2} (Sonawane et al., 2018a). Vulcan XC-72 (Cabot) was used as support for FePc, and the FePc/C catalyst was synthesized by the procedure detailed by Khan M. D et al. (2021). The filtered FePc/C catalyst was washed repetitively using deionized water to remove most of the H_2SO_4, followed by a 12 h oven drying at 110°C. Pyrolysis of the catalyst was neglected. In order to prepare the catalyst ink, Nafion (10 wt %) was used as a binder, and finally, the catalyst ink was sprayed onto the GDL carbon paper until the desired loading (0.75 mg cm^{-2}) was achieved.

Set-Up and Operation of the Reactor

In the experimental work, the single-chamber microbial fuel cells (SMFCs) were made up of glass chambers (300 ml) maintained anaerobically during operation as shown in **Figure 1**. The bare SSFF and PANI fabricated SSFF (PANI–SSFF) were employed as anodes in unmodified (SSFF–MFC) and modified (PANI–SSFF–MFC) SMFCs, respectively, and carbon paper (16 cm^2) coated with FePc/C were used as air cathodes in both the SMFCs. Cathodes and a cation exchange membrane (CEM, Fumasep FKB-PK-130, Fumatech, Germany) were attached to the glass chambers' outside the surface, having a 4 cm opening. The space between both the electrodes was 5 cm. Current collectors made of stainless steel mesh (16 cm^2) were used in conjunction with cathodes in both the SMFCs. To complete the circuit, a titanium wire was utilized to connect both electrodes using a 1,000 Ω external resistance. Both the SMFCs were inoculated with a microbial consortium from the anodic chamber of another running SMFC (Khan M. D et al., 2021) that was initially inoculated with the sludge collected from Tudhoe mills wastewater treatment plant (Durham, United Kingdom) and was operated for more than 3 months containing AB29 azo dye and acetate. Each SMFC had a 250 ml effective working volume, with AB29-containing wastewater being fed in a 4:1 ratio with anaerobic sludge. The anolyte medium was 50 mM phosphate buffer (pH 7.2) along with minerals and vitamins (Fontmorin et al., 2018), and sodium acetate (1 g L^{-1}) was fed as a carbon source/electron donor during the operation. The SMFC's headspace was filled with N_2 gas in addition to sparging the anodic content with N_2 gas (20 min). In this study, for feasibility testing, AB29 (200 mg L^{-1}) was introduced to the SMFC with 1 g L^{-1} acetate. The SMFCs were maintained at a pH of 7.2–7.7 during the experiments, and the experiments were conducted in a box having controlled temperature (30 ± 1°C), in the dark, and in duplicate. After AB29 was anaerobically treated in SMFCs, the intermediates generated (aromatic amines) after degradation of AB29 were transferred and subsequently treated in 200 ml glass aerobic bioreactors containing SMFC effluent (150 ml) and acclimated aerobic sludge (50 ml) for 36 h (**Figure 1**). Air stone spargers attached with aquarium pumps were used to maintain the required level of dissolved oxygen in aerobic bioreactor contents. The decolorization studies of azo dyes were conducted in anaerobic conditions using acclimated anaerobic sludge and modified and unmodified anodes were conducted at the open circuit for comparison.

Voltage Generation and Acid Blue 29 Biodegradation

The voltage generated in both the SMFCs across external load was measured using USB-6225 multifunction I/O device, National Instruments, United States data logger. Using the equations reported in Sultana et al. (2015), the power density (mW m^{-2}) and Coulombic efficiency (CE) were calculated (Sultana et al., 2015). After collecting the samples during the combined operation, they were centrifuged for 30 min at a speed of 5,000 rpm, followed by filtration using a PTFE membrane of size 0.22 µm. The collected samples were scanned in a UV–Vis spectrophotometer (JENWAY 7315, United Kingdom) over the entire wavelength range of 200–700 nm, and the deviation in AB29 concentrations was calculated by measuring the deviation in absorbance at λ_{max} = 602 nm (–N=N–) to confirm the AB29 decolorization. Absorbance values were then converted to the concentration values using a calibration graph. Before the SMFC experiment, an adsorption test on fresh SSFF was also performed and was found to be negligible. Generally, the ionic dyes in an aqueous solution will dissociate almost completely (solubility range 100 mg L^{-1} to 80,000 mg L^{-1}), therefore, no precipitation was observed.

To evaluate the organic removal during combined operation, HACH COD test kits and a spectrophotometer (DR6000, HACH Company, United States) were used to measure the COD of filtered samples. **Eq. 1** was used to determine the decolorization efficiencies in both SMFCs, **Eq. 2** was used to explain the kinetics of AB29 decolorization, and **Eq. 3** was used to calculate the COD removal efficiencies (RE) in integrated set-ups.

$$\text{Decolorization efficiency } (\%) = \frac{(A_0 - A)}{A_0} * 100 \quad (1)$$

$$A = A_0 e^{-kt} \quad (2)$$

$$\text{COD RE}\,(\%) = \frac{(B_0 - B)}{B_0} * 100 \quad (3)$$

Here, A_0 and A represent AB29 concentrations, and B_0 and B represent COD at times "t_0" and "t", respectively.

Electrochemical Characterization

Using a variable resistance box, polarization curves for both the SMFCs were acquired by increasing the external loads from 20 to 5,000 Ω. Power densities were calculated, and curves were drawn using obtained data. An AutoLab potentiostat (PGSTAT204, Metrohm, the Netherlands) was used for performing cyclic voltammetry (CV), galvanostatic charge-discharge (GCD), and electrochemical impedance spectroscopy (EIS). The CV tests of abiotic anodes were carried out in H_2SO_4 (0.5 M) in the −0.2–1.0 V (vs. Ag/AgCl) range at 10 and 25 mV s^{-1} scan rates, whereas GCD was conducted from −0.2 and 1.0 V (vs. Ag/AgCl) in a phosphate buffer (50 mM) at 1 mA cm^{-2} current density. Abiotic PANI–SSFF or SSFF anode was used as working electrode, and an Ag/AgCl (+0.205 V vs. SHE) and a Pt mesh were worked as reference and counter electrodes, respectively. EIS tests for SMFCs were conducted in a two-electrode configuration from 100 kHz to 0.01 Hz frequency range using an AC perturbation of 10 mV at open circuit potential, where anode worked as both reference and counter electrode and cathode served as the working electrode. To better understand PANI's role as an anode modifier, the specific capacitance of SSFF and PANI-SSFF was measured and calculated using **Eq. 4**.

$$C_S = \frac{I*t}{V*A} \quad (4)$$

.

The charge-discharge current, discharge time, potential window, and anode area are represented by I, t, V, and A, respectively.

Analysis of Degradation Products

The gas chromatograph (GC, 7890B) (Agilent, United States) having HP-5 column (30 m × 0.25 mm I.D. x 0.25 μm film thickness) in combination with a mass detector (5977B) (Agilent, United States) were utilized to analyze samples collected during the combined operation. Degraded samples (2 ml) were extracted in a 1:1 ratio with ethyl acetate and then exposed to the air to evaporate the ethyl acetate. The final analysis was performed by dissolving dried samples in methanol (1 ml). The program used for the GC-MS analysis was reported in Khan M. D et al. (2021).

Surface Characterization by Scanning Electron Microscopy

The SEM (JEOL JSM-5600LV) was used to characterize the surface of abiotic anodes and bioanodes. Bioanodes were analyzed by SEM to observe biofilm formation on their surface. Small pieces of bioanodes were cut and left overnight in Sorenson's phosphate buffer containing 2% glutaraldehyde, followed by two rinses in a phosphate buffer (pH 7.2) before SEM analysis was performed. After that, the samples were rinsed with various grades of ethanol solution (25, 50, 75, and 100%). A Baltec CPD (critical point dryer) was used to dry samples in order to get clear micrographs.

DNA Extraction, Sequence Data Processing, and Analysis

According to the manufacturer's instructions, the DNA from the inoculum, suspension, and anodic biofilm was extracted using the Fast DNA Spin Kit (MP Biomedicals, United States). Nanodrop (ThermoFisher, United Kingdom) was used to assess the quality and concentration of the extracted DNA samples, which were stored at −80°C. Using primers 515F and 806R, which target the 16S rRNA V4 region, PCR amplification was done to sequence bacterial communities (Caporaso et al., 2011). The standard protocol for 16S sequencing, processing of sequenced data, and statistical analysis was described by Khan M. D et al. (2021). According to the process reported by Shamurad et al. (2019), phylogenetic trees were built in this study.

RESULTS AND DISCUSSION

Bioelectricity in Single-Chamber Microbial Fuel Cell

To examine the cell performance of both PANI–SSFF and SSFF anodes, two SMFCs (PANI–SSFF–MFC and SSFF–MFC) were operated containing AB29 (200 mg L^{-1}) and carbon source (acetate, 1 g L^{-1}) in 50 mM phosphate buffer along with required mineral and vitamins. Three cycles for PANI–SSFF–MFC and seven cycles for SSFF–MFC were carried out with 1,000 Ω resistance at 30 ± 1°C to grow biofilm on the anode. **Figure 2A** showed the cell potential variations obtained with PANI–SSFF and SSFF anodes over 13 and 30 days start-up periods, respectively. The maximum cell potential achieved in the first cycle for PANI–SSFF–MFC and SSFF–MFC were 123 and 17 mV, respectively. It should be noted that by adding fresh media in the successive batch cycles, the maximum cell potential reached 235 and 236 mV in the second and third cycle with the PANI–SSFF anode and 105 and 107 mV in the last two cycles with SSFF anode which confirmed the stability of the cells. The start-up period was reduced by 57% from 30 days in case SSFF–MFC to 13 days for PANI–SSFF–MFC. With the PANI-SSFF anode, a faster start-up time was accomplished as a result of its high biocompatibility with electrogenic bacteria performing electron transfer to the anode extracellularly. The results in this study showed that as a result of the presence of the PANI coating, the start-up time of the PANI–SSFF anode was reduced. Similar results were also reported by Lai et al. (2011), where using an external resistance of 510, the cell voltage of the PANI modified MFC was 380 mV, while

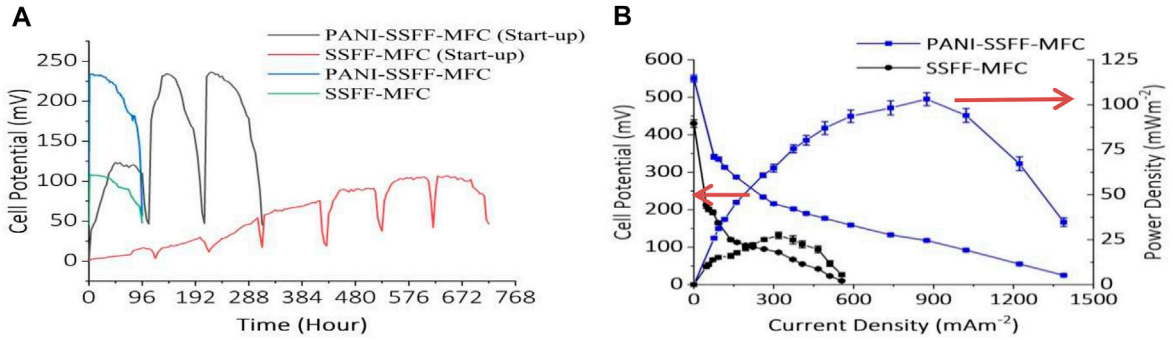

FIGURE 2 | (A) Output cell potential of the SMFCs during the start-up period, and voltage generation from SMFCs during the final experiment and **(B)** polarization and power density curves of the PANI-SSFF-MFC and SSFF-MFC containing AB29 (200 mg L^{-1}) and acetate (1 g L^{-1}) in 50 mM phosphate buffer.

the unmodified MFC was 290 mV. The start-up time was shortened by 33.3% from about 6 to 4 days. As shown in **Figure 2B**, PANI–SSFF–MFC showed an enhancement in the bioelectricity generation. With 1,000 Ω external resistance, the maximum cell potential of PANI–SSFF–MFC was 234 mV, while that of SSFF–MFC was 108 mV after 96 h of operation treating 200 mg L^{-1} azo dye with acetate (1 g L^{-1}). The reason for low cell potential in the case of SSFF–MFC is that the SSFF biocompatibility is not as good as that of the PANI–SSFF anode even after 30 days of start-up. On the SSFF, a limited quantity of bacteria was grown as a result of the small reactive surface area of the SSFF, resulting in a low rate of electron transfer. However, after the modification of SSFF with PANI, the performance of PANI–SSFF has been improved substantially. PANI–SSFF anode offered alluring incorporation of the biocompatibility, low activation overpotential due to its conductivity and the high specific surface area, and these attractive qualities facilitated the transfer of electrons at the anode-biofilm interface. The voltage curve was dropped sharply in both MFCs at the end of every cycle, which ascribed to the depletion of acetate. **Figure 2C** presented the power density and polarization curves of PANI–SSFF–MFC and SSFF–MFC and were monitored during the last cycle of their startup-up periods when cell potential was the highest. **Figure 2C** showed that the power density significantly enhanced after modification of anode with PANI. The maximum power density achieved for PANI–SSFF–MFC was 103 ± 3.6 mW m^{-2}, while in the case of SSFF–MFC highest power density attained was 27 ± 1.7 mW m^{-2} normalized by anode area. The outcomes revealed that the power density in the case of PANI–SSFF–MFC increased to 3.8 times compared to that of SSFF–MFC. The performance improvement is ascribed to the PANI coated on SSFF that reduced the start-up time of the PANI–SSFF–MFC, as evident in the higher voltage production from day 1. Many researchers have also reported enhancement in power output after PANI modification (Mehdinia et al., 2013; Hou et al., 2015; Sonawane et al., 2018b; Xu P. et al., 2020). In our previous work (Khan M. D et al., 2021), where SMFC was treating 200 mg L^{-1} AB29, the highest power density reached was 56 ± 2.7 mW m^{-2}; however, in the present study, the maximum power density was 84% higher due to the presence of PANI on the anode surface which improved the bioanode activity and ultimately the performance of SMFC. The conductive PANI coating conforms to the SSFF morphology without altering its porous structure; thus, the macropores of the resulting anode allow bacteria colonization in the electrode's internal structure, enhancing the biofilm, and electrode interaction.

Decolorization Studies of Azo Dye

During the biodegradation of azo dyes, the first step is decolorization, wherein electrons released from electron donor or co-substrate as a result of oxidation are utilized by azo dyes to cleavage their azo bonds. On the other side, the presence of the anode promotes the production of electrons by accelerating the metabolism of the electron donor, which ultimately increases the rate of dye reduction. The crucial stage in determining the decolorization performance of MFCs is generating electrons in the MFCs and transferring them to azo dyes. In our study, once the MFCs reached a state of stability following the start-up phase, 96 h of experiments were performed to examine the decolorization efficiency in MFCs with fabricated (PANI–SSFF) and bare (SSFF) anodes in the following state: 200 mg L^{-1} AB29, 1g L^{-1} acetate, 1,000 Ω external resistance, and 30 ± 1°C temperature. As presented in **Figure 3A**, the decolorization efficiencies in PANI–SSFF–MFC and SSFF–MFC were 51 ± 3% and 38 ± 3%, respectively, after running for 24 h due to faster consumption of acetate at the anode and as the operating time extended to 96 h, the decolorization efficiencies reached 93 ± 3% and 82 ± 2% in PANI–SSFF–MFC and SSFF–MFC, respectively. The better decolorization effect in the case of PANI–SSFF–MFC indicated that the PANI–SSFF anode performed well, and the conductive coating on SSFF can be used to enhance MFCs' performance. The PANI-SSFF anode exhibited a much greater affinity for bacteria than SSFF, which accelerated bacterial adhesion and growth on the anode surface. Therefore, the biofilm generated on the PANI-SSFF surface swiftly transferred a large number of electrons from the oxidation of acetate to the anode surface and AB29 via an electron transfer chain. Consequently, highly efficient decolorization by reducing azo bonds of azo dyes was accomplished with high power generation (Xu H. et al., 2020). For the open circuit controls, the efficiency of AB29 decolorization was 51 ± 1.2% for the open circuit PANI–SSFF–MFC and 50 ± 1.3% for the open circuit SSFF–MFC. This suggested that in the bioelectrochemically active environments, SMFC-anode-mediated reducing equivalent transfer to the azo moiety was more efficient

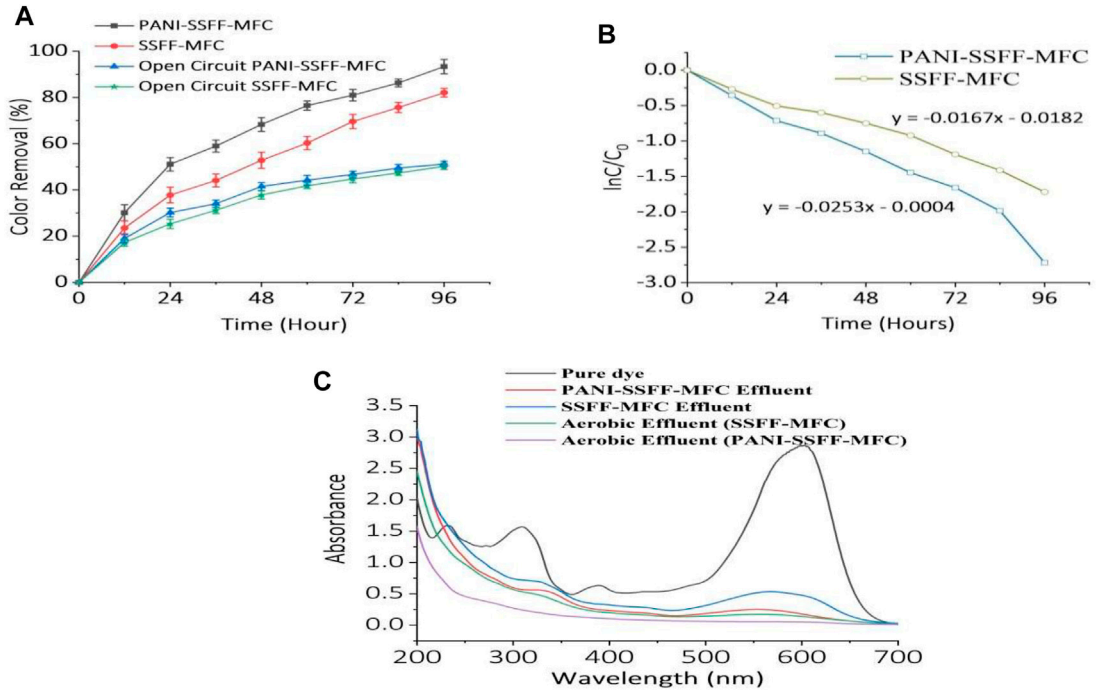

FIGURE 3 | (A) Decolorization of AB29 (200 mg L^{-1}) with time **(B)** decolorization kinetics in SMFCs and **(C)** UV-Vis absorption spectra for pure dye and effluent from SMFCs.

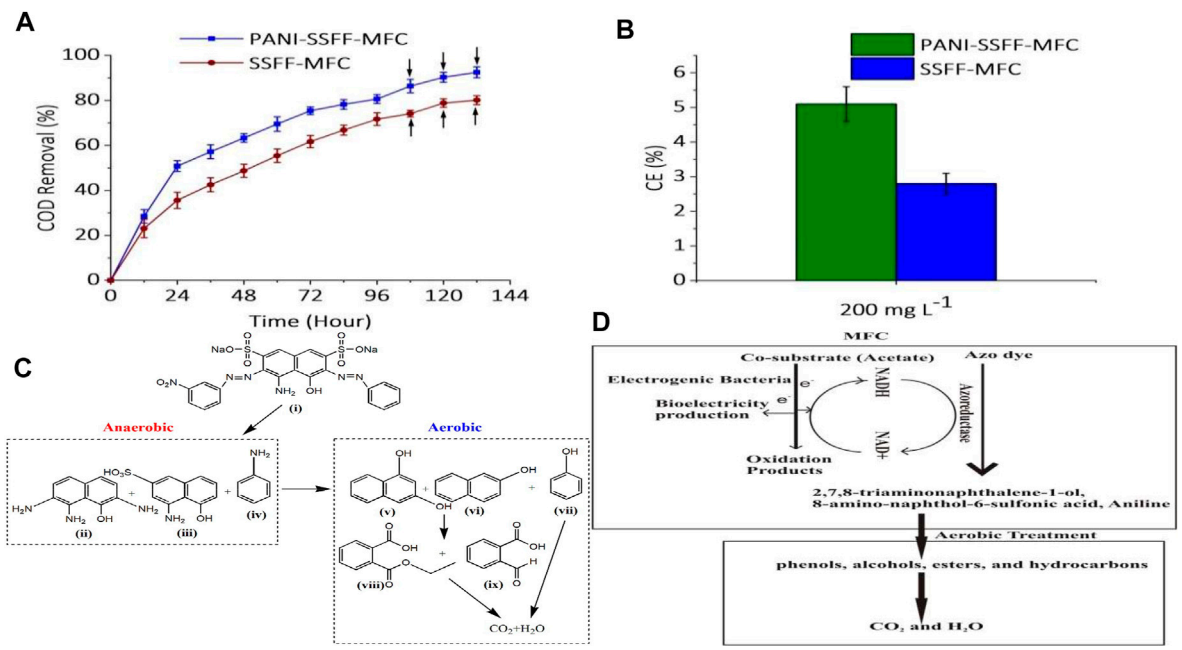

FIGURE 4 | (A) COD removal (following successive aerobic treatments, the COD removed was displayed by arrows); **(B)** CEs in SMFCs **(C)** proposed degradation pathway of AB29 in PANI–SSFF–MFC–aerobic bioreactor set-up and **(D)** mechanism of AB29 degradation in PANI-SSFF-MFC-aerobic bioreactor treatment system.

than open circuit controls, owing to lower efficiencies. Since open circuit controls lack an anode, they are equivalent to anaerobic bioreactors, which use alternate terminal electron acceptors. Moreover, the logarithmic relationship of AB29 concentration with time is presented in **Figure 3B**. The rate constant for PANI–SSFF–MFC (0.0253 h^{-1}) was 1.5 times more than that of

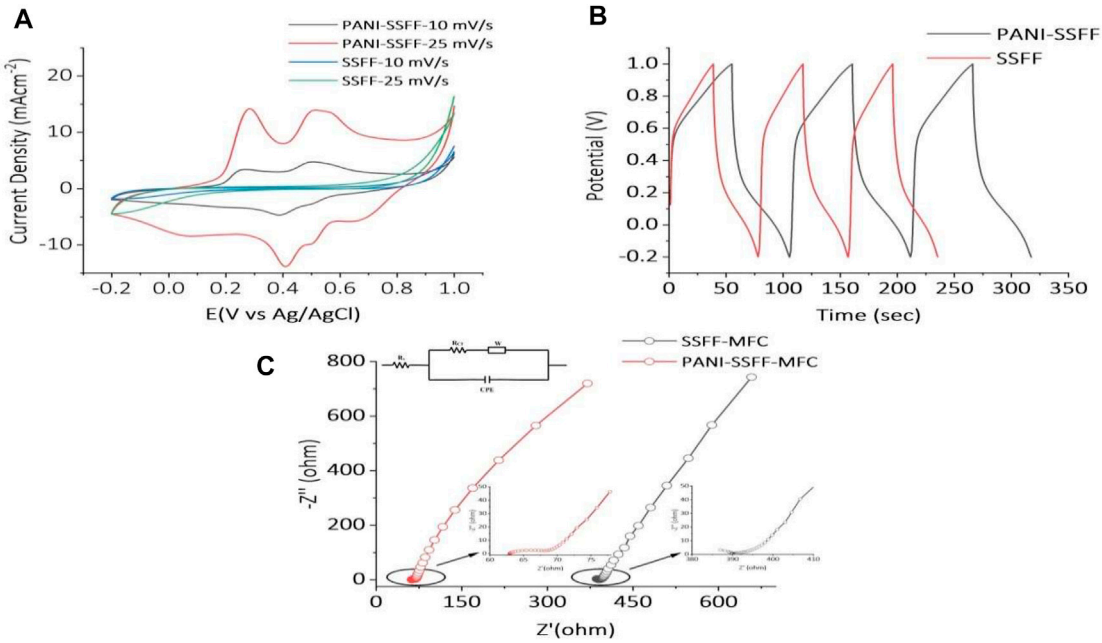

FIGURE 5 | (A) CV curves of PANI–SSFF and SSFF anodes; **(B)** GCD tests for PANI–SSFF and SSFF anodes; and **(C)** Nyquist plots of impedance spectra and circuit diagrams of the SMFCs.

SSFF–MFC (0.0167 h^{-1}), and the AB29 decolorization kinetics followed the pseudo-first-order kinetic model. In our previous work (Khan M. D et al., 2021), the rate constant was 0.0136 h^{-1}, which was 1.86 times less than the present study for PANI–SSFF–SMFC treating 200 mg L^{-1} dye, confirming the presence of PANI coating on the SSFF anode increased the decolorization rate by accelerating the activity of the bioanode.

To analyze the decolorized intermediates of AB29 in the SMFC reactors, samples collected at definite intervals were scanned in the entire wavelength range (200–700 nm) of the UV-Vis spectrophotometer. The UV-Vis spectra of the pure AB29 sample, PANI–SSFF–MFC, SSFF–MFC treated effluent, and aerobically treated samples are presented in **Figure 3C**. The AB29 pure sample showed four distinguishable peaks; 232 nm-benzene ring, 309, 389 nm–naphthalene rings, and 602 nm- azo link. Anaerobically treated samples showed some absorption peaks indicative of biodegraded products (aromatic amines). The disappearance of any typical absorption peak in the aerobically treated samples (for PANI-SSFF-MFC effluent) indicated that AB29 was fully biodegraded in an integrated PANI-SSFF-MFC–aerobic bioreactor treatment process. However, some peaks were present in the aerobically treated samples (for SSFF-MFC effluent), indicating that AB29 was not fully biodegraded, and there could be the possibility of the presence of aromatic compounds.

Degradation Studies of Acid Blue 29 in an Integrated Set-Up

In order to further investigate the efficient biodegradation of AB29 by SMFC–aerobic bioreactor treatment method, the COD removal efficiency of AB29 during the combined operation was monitored (**Figure 4A**). The COD of influent was 1,007 mg L^{-1} (AB29–227 mg L^{-1} and acetate - 780 mg L^{-1}). Similar to the decolorization performance, the COD removal efficiencies were also increased with operating time. In the initial 24 h, the co-substrate had been consumed faster in case of PANI–SSFF anode due to faster bacterial activity; therefore, the COD removal efficiency of PANI–SSFF–MFC reached 51 ± 2.4%, higher than SSFF–MFC (36 ± 3.6%). PANI–SSFF–MFC had the higher output power, which showed that more microbes on the anode surface oxidized the acetate to discharge electrons. Consequently, there were more electrons to be utilized to break the azo bonds, which again resulted in the higher COD removal efficiency of AB29 in PANI–MFC after 96 h of operation, which was 81 ± 2%, while it was 72 ± 3% for SSFF–MFC. Based on the COD removed/unit time, the values were 8.5 and 7.5 mg L^{-1} h^{-1} for PANI–SSFF–MFC and SSFF–MFC, respectively. Under anaerobic conditions, sulfonated aromatic amines and aniline were formed due to the breaking of the azo bonds of AB29, inhibiting further biodegradation (Liu et al., 2017). These intermediates formed after decolorizing AB29 contributed somewhat to a certain quantity of COD since acetate had depleted entirely at the end of SMFC operation. The effluents of both MFCs with residual organic matter were supplied to the aerobic bioreactor for further COD removal. The COD removal in the aerobic bioreactor was contributed by the aerobes, which can hydrolyze and oxidize organic matters (Gutu et al., 2021). The final COD removal efficiencies for PANI–SSFF–MFC and SSFF–MFC were 92.5 ± 2% and 80 ± 2%, respectively, after treatment of effluent of both the MFCs for 36 h aerobically.

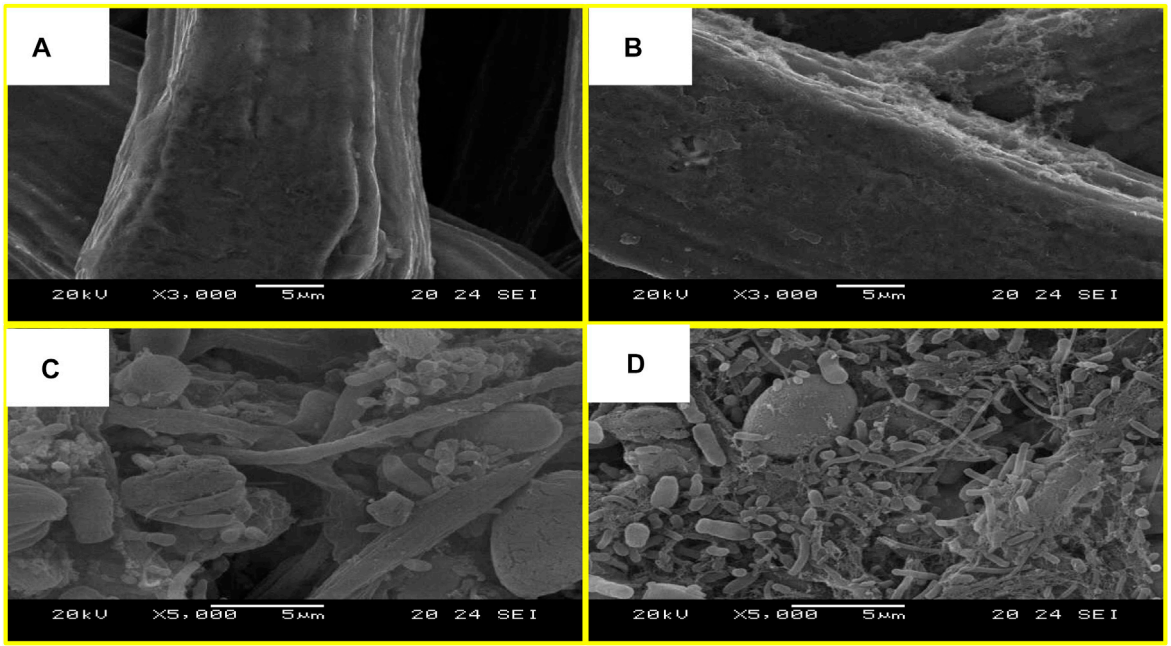

FIGURE 6 | SEM micrographs of the **(A)** SSFF, **(B)** PANI–SSFF, **(C)** biofilm on the SSFF, and **(D)** biofilm on the PANI–SSFF at magnifications of 5,000x.

Figure 4B showed the CEs calculated for both SMFCs. This study suggested that all the acetate quantity used by SMFC was not converted to biogenic electricity production. The SMFCs showed low CEs based on the anodic process because both AB29 decolorization and the bioelectricity generation processes would compete for electrons since both processes required electrons. In additiion, the existence of alternate electron acceptors, for example, SO_4^{-2} and competing reactions (methanogenesis and fermentation) as well as the inhibitory nature of AB29 and intermediates, can also affect the CEs. At a 200 mg L^{-1} dye concentration, the CE was noted to be comparatively higher in the case of PANI–SSFF–MFC, and it was found to be 5.1 ± 0.5%, while for SSFF–MFC, it was 2.8 ± 0.3%. The higher CE in PANI–SSFF–MFC could be due to the more pronounced biofilm on the large biocompatible surface area of PANI–SSFF that promoted electron transfer rate, thus further enhancing the degradation efficiency of the PANI–SSFF–MFC. The CE was higher than the value mentioned in our previous work (Khan M. D et al., 2021), where AB29 (200 mg L^{-1}) was treated in an SMFC using a carbon brush anode in the presence of acetate (1 g L^{-1}), and it was 3 ± 0.3%. The values were considerably higher than those reported by previous researchers, who reported a decrease in CEs after inoculating SMFCs with a mixed culture sludge (Fang et al., 2015; Sultana et al., 2015; Song et al., 2017; Oon et al., 2018).

The pathway of degradation is very significant to ensure the effective mineralization of azo dyes and to analyze the type and characteristics of biodegraded intermediates. The intermediate products formed after biodegradation of AB29 in combined PANI–SSFF–MFC–aerobic bioreactor set-up were examined utilizing the GC-MS technique, and the proposed AB29 degradation pathway is presented in **Figure 4C**. Azoreductase enzymes in anaerobic conditions are accountable for the reductive breakdown of azo bonds of azo dyes (Song et al., 2017), while aerobic degradation of anaerobic products occurs due to the presence of oxidoreductases in aerobic bioreactors under aeration. In the present study, we found that 2,7,8-triaminonaphthalene-1-ol (m/z = 190) 2), 8-amino-naphthol-6-sulfonic acid (m/z = 239) 3) and aniline (m/z = 93) 4) were formed after reductive breakdown of azo bonds of AB29 (MW = 616.49). Al-Tohamy et al. (Al-Tohamy et al., 2020) also reported the formation 2,7,8-triaminonaphthalene-1-ol after degradation of diazo reactive black 5 by *Sterigmatomyces halophilus* SSA1575. It has been earlier demonstrated that several aerobic microbes can transform recalcitrant aromatic amines into phenols, alcohols, esters, and hydrocarbons, which are finally mineralized into CO_2 and H_2O by the action of oxygenase (Zhong et al., 2018; Bhandari et al., 2021). During the aerobic treatment process in this study, deamination of 2,7,8-triaminonaphthalene-1-ol, 8-amino-naphthol-6-sulfonic acid and aniline into 1,3- naphthalenediol (m/z = 160) 5), 2-naphthol (m/z = 144) 6) and phenol (m/z = 94) 7) possibly occurred which were further transformed into monoethyl phthalate (m/z = 194) 8) and 2-formylbenzoic acid (m/z = 150) 9). In our previous work (Khan M. D et al., 2021), a similar degradation pathway was also observed where AB29 was first converted into amines (8-amino-naphthol-3,6-disulfonic acid and 2,8-diamino-1-naphthol) in SMFC and finally into smaller compounds (pthalic acid and diethyl phthalate) after aerobic treatment. A detailed mechanism of azo dye AB29 degradation in PANI-SSFF-MFC-aerobic bioreactor treatment system has been presented in **Figure 4D**.

Electrochemical Analysis of Electrodes and Single-Chamber Microbial Fuel Cell

The CVs obtained for the SSFF and PANI–SSFF in 0.5 M sulfuric acid at a scan rate of 10 and 25 mV^{-1} are shown in **Figure 5A**. The voltammograms of SSFF did not show any typical redox peak. However, PANI–SSFF exhibited significant redox peaks (vs. Ag/AgCl). The PANI undergoes a reversible transformation into semiconducting leucoemeraldine and conducting emeraldine forms, producing redox peaks and pseudocapacitance (Ansari et al., 2016). It has been previously stated that the PANI generally presents two pairs of redox peaks, representing redox transitions of the PANI (leucoemeraldine-emeraldine and emeraldine-pernigraniline transitions) in acid solution when performed on glassy carbon electrode (Yuan et al., 2011; Obaid et al., 2014). In this study, however, only one pair of peaks was detected, probably due to the relatively high anode surface area (9 cm^2), which served as a working electrode (Yuan et al., 2011), leading to superimposition of the peaks. Furthermore, the PANI–SSFF had larger current densities of redox peaks than the SSFF. The PANI film coated on SSFF having good conductivity also reduced the start-up time of the biofilm formation and enhanced electron transfer rate, which was also confirmed by cell potentials (**Figures 5A andB**). Additionally, the area surrounded by CV curves for the PANI–SSFF anode depicted a higher specific capacitance for the PANI–SSFF anode consistent with GCD results.

The GCD is a convincing process to evaluate the electrochemical performance of any material in a specific condition. **Figure 5B** exhibited GCD curves of the SSFF and PANI–SSFF for the initial three cycles. The specific capacitance calculated using the second cycle increased to 0.04 F cm^{-2} for abiotic PANI–SSFF anode compared to abiotic SSFF anode (0.032 F cm^{-2}). This suggested that PANI coating on the SSFF had a considerable impact on promoting the electrochemical charge storage capabilities of the SSFF surface. The PANI is a highly conductive material with many electrons, which increases electron cloud displacement and hence the charge-discharge time. The PANI utilizes more Coulombic forces as the charge-discharge time increases, resulting in a reduction in resistance as the charge transfer process improves; as a result, the PANI–SSFF anode's charge-storage capacity increases significantly (Yuan et al., 2011).

To reveal the electrochemical processes occurring in the system, the EIS functions as an essential analytical tool. To acquire a quantitative explanation for deviation in impedance which is accountable for the change in color removal efficiency and generation of biogenic electricity in PANI–SSFF–MFCs and SSFF–MFCs, the response of both the MFCs was studied using the EIS technique during the last cycle of their start-up periods when the systems were stable. The equivalent circuit has been presented for both the SMFCs represented charge transfer resistance (R_{ct}), solution or ohmic resistance (R_s), diffusion element (Zd), and constant phase element (CPE). **Figure 5C** showed the EIS spectra of PANI–SSFF–MFC and SSFF–MFC. Due to the varied anodes used in the MFCs, a considerable variation was detected. The R_s stands for electrode materials' inherent resistance, contact resistance at the active materials' surface, and ionic resistance of electrolytes (Quan et al., 2018). R_s measured for PANI–SSFF–MFC was lower (62.8 Ω) as compared to SSFF–MFC (380 Ω) due to minor opposition to the electrons flow across the electrodes and connections; however, R_{ct} of both the anodes were comparable possibly because of the longer duration of SSFF–MFC start-up. The considerable reduction in resistance values for PANI–SSFF–MFC suggested the decrease in resistance of electrochemical reaction and electron transfer rate.

Microscopic Studies

The surface morphology of abiotic anodes and bioanodes has been studied by SEM. **Figures 6A,B**, showed SEM images of abiotic SSFF and PANI–SSFF. **Figure 6A** displayed the smooth surface of SSFF, which is a decent substrate for modification and can be utilized for MFC applications because of its conducting, solid, and porous structure; however, due to biocompatibility issues; SSFF was fabricated with PANI in this study. **Figure 6B** showed a densely packed layer of PANI on the SSFF. The structure resulting from PANI modification enhanced the accessible anode area, which accelerated strong biofilm development on the anode favoring efficient extracellular electron transfer (EET).

Figures 6C,D showed the SEM images of SSFF and PANI–SSFF bioanodes at the end of SMFCs operation and displayed the existence of bacterial communities on both the bioanodes. However, the bacterial community differed broadly for PANI–SSFF and SSFF bioanodes in terms of type and dominance. Both the bioanodes displayed the existence of a diversity of microbes, with mainly the spherical community on SSFF bioanode (**Figure 6C**). On the other hand, in the case of the PANI–SSFF bioanode, the rod-shape bacteria that produced hairlike structures, called pili, were uniformly grown and can perform the transfer of electrons even not in direct contact with the anode surface (**Figure 6D**) (Sun et al., 2010; Aiyer, 2020). It is also described that biofilm development on the surface of anode could limit the HSO^{4-} doped PANI to be de-doped (Lai et al., 2011). Uniformly adhered microbes on PANI–SSFF bioanode were responsible for both higher azo dye decolorization rate and power densities (Sun et al., 2012). Microbial community investigation can show the importance of morphologies and can explain their function.

Microbial Community Analysis

It is crucial to analyze the microbial community of bioanode and suspension of SMFCs to understand their role in dye decolorization and bioelectricity generation. Different types of microbes such as exoelectrogens, dye degrading, fermentative, and electricians having specific roles can function together to define the overall functioning of the SMFCs. **Figures 7A,B** illustrate the phylum and genus-level variation in the community of microbes in the suspension and biofilm relative to the inoculum. The phyla *Proteobacteria* (30%), *Planctomycetes* (17%), *Chloroflexi* (16%), *Bacteroidetes* (12%), *Actinobacteria* (9%) and *Verrucomicrobia* (7%) were dominated in the initial inoculum (**Figure 7A**). At the end of MFC experiments treating 200 mg L^{-1} dye-containing acetate (1g L^{-1}), *Proteobacteria* (72, 58%), *Bacteroidetes* (15, 15%), *Acidobacteria* (5, 10%), and *Firmicutes* (5, 9%) were the most abundant phyla covering 97

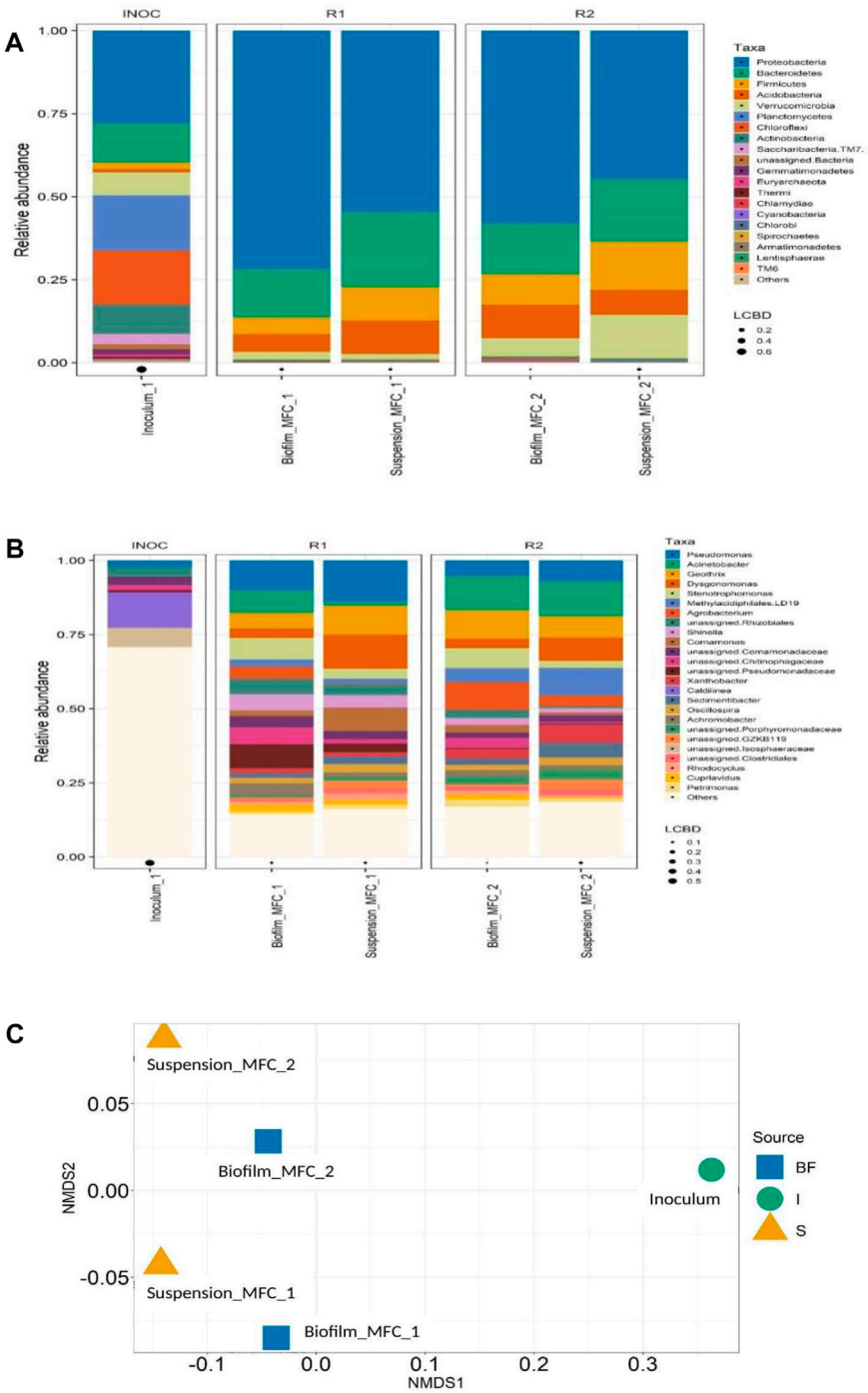

FIGURE 7 | Relative abundance of the microbial community at the **(A)** phylum, **(B)** genus level, and **(C)** NMDS plot (BF–biofilm, I–inoculum, S–suspension; MFC_1–PANI–SSFF–MFC; MFC_2–SSFF–MFC) and **(D–F)** phylogenetic distance trees of key bacterial taxa in MFCs and close relatives. **(D)**–*Proteobacteria*; **(E)**–*Bacteroidetes*; **(F)**–*Firmicutes*.

and 92% of the biofilm microbial community of PANI–SSFF and SSFF anodes, respectively, whereas, in suspension, *Proteobacteria* (55, 45%), *Bacteroidetes* (23, 19%), *Acidobacteria* (10, 7.5%) and *Firmicutes* (10, 14.5%) covering 98 and 86% of the microbial community were the dominant phyla in PANI–SSFF–MFC and SSFF–MFC, respectively. In our previous work (Khan M. D et al., 2021), *Proteobacteria*, *Bacteroidetes*, and *Firmicutes* covering 88.1% in biofilm and 81.2% in suspension were also the dominating phyla that encouraged decolorization as well as bioelectricity generation. *Proteobacteria* and *Bacteroidetes* have

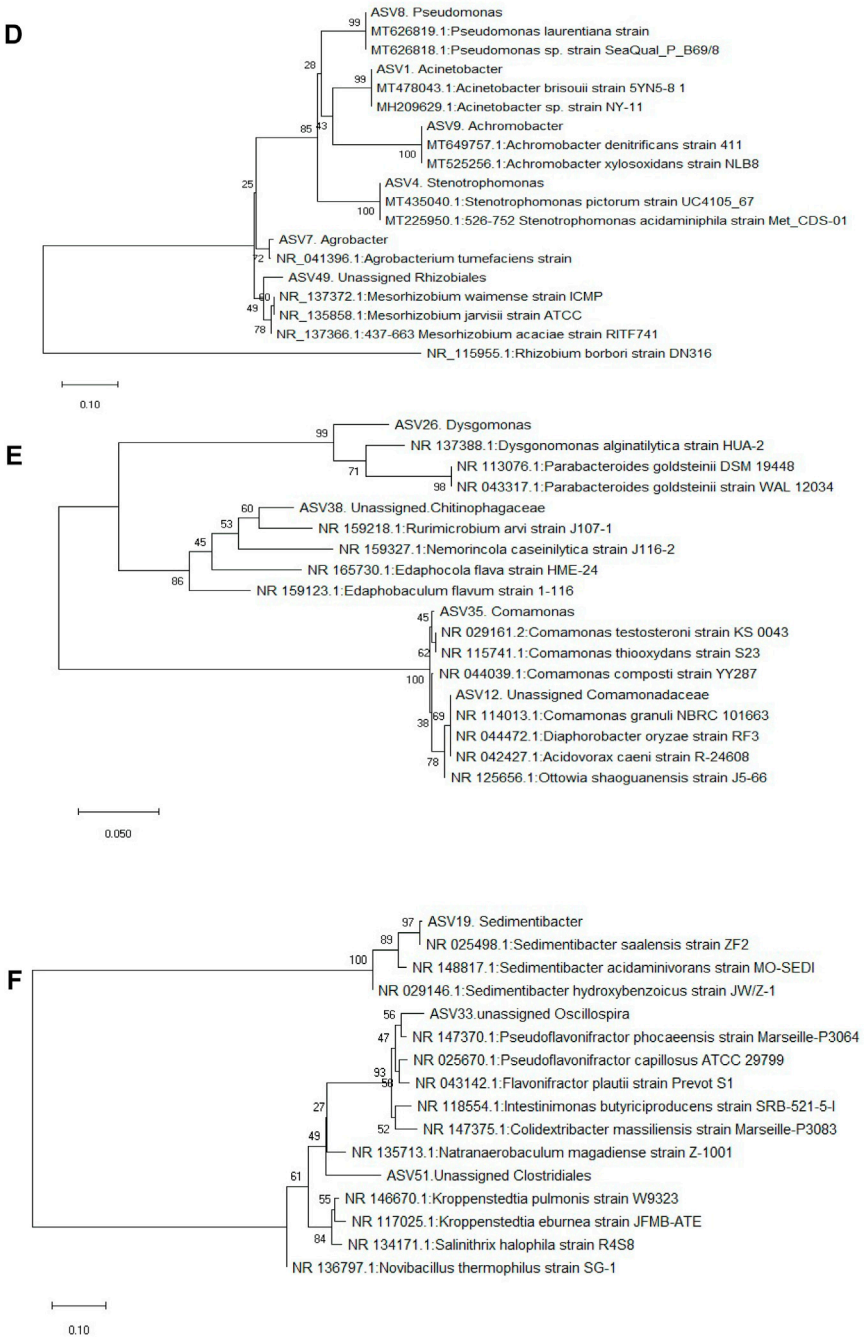

FIGURE 7 | (Continued).

been reported to be the key communities which are potential exoelectrogens on the bioanodes that promote bioelectricity generation and degrade various azo dyes (Ruiz et al., 2014; Quan et al., 2018; Cao et al., 2019), which also encouraged AB29 decolorization and biogenic electricity production in this study. In the present study, a higher abundance of *Proteobacteria* was detected in biofilm and suspension of PANI–SSFF–MFC, whereas the abundance of *Bacteroidetes* was higher on SSFF biofilm; however it was lower in the suspension of SSFF–MFC as compared to PANI–SSFF–MFC. In both MFCs, *Firmicutes* were also observed in higher abundance and efficient to transfer electrons extracellularly and decolorizing azo dyes (Fernando et al., 2013). These three phyla enriched in the anodic chamber of MFCs contain several types of electrochemically active bacteria (EAB), which are reported to be involved in treating azo dyes and transferring electrons to the anode for bioelectricity generation (Quan et al., 2018; Wang et al., 2018; Rathour et al., 2019). The other communities present in the biofilm were *Verrucomicrobia*

(2.3%, 5.4%), *Actinobacteria* (0.6%, 1%), and communities present in suspension were *Verrucomicrobia* (1.7%, 13%) of PANI-SSFF-MFC and SSFF-MFC, respectively. The phylogenetic trees (**Figures 7D–F**) showed the most dominant genera from *Proteobacteria*, *Bacteroidetes*, and *Firmicutes*, along with close relatives chosen from random BLAST searches of the Genbank database.

From **Figure 7B**, *Pseudomonas* was found to be present in higher abundance in PANI–SSFF–MFC (biofilm–10.2%; suspension–14%) and was responsible for the production of biogenic electricity through the excretion of redox mediators that transferred electrons to the anode extracellularly (Yang et al., 2012) and also capable of degrading azo dyes (Ge et al., 2015). *Acinetobacter* use acetate as a growth substrate and was present in high abundance on bioanodes of both the SMFCs (PANI–SSFF–MFC–8%; SSFF–MFC–11%), and contributed significantly to the decolorization of dyes and electricity production (Chen et al., 2010; Chen et al., 2018). *Stenotrophomonas* was present in higher abundance in PANI–SSFF–MFC (biofilm–7.3%; suspension–3.4%), which was able to degrade AB29, which is consistent with higher decolorization efficiency in PANI–SSFF–MFC (Dai et al., 2020). *Geothrix* is a known EAB of *Acidobacteria* phylum and has the ability to utilize an electrode as the electron acceptor (Yaqoob et al., 2021), which was present in both the SMFC. *Dysgonomonas* has been reported to produce biogenic electricity and biodegrade azo dye (Gao et al., 2014; Xie et al., 2016), which was found to be more abundant in the suspension of PANI–SSFF–MFC (11%), favoring better performance. *Rhizobiales* were also present in higher abundance in PANI–SSFF–MFC (biofilm–5.3%; suspension–3.5%) as compared to SSFF–MFC (biofilm–2.7%; suspension–0.6%), which accelerated the biofilm formation on PANI–SSFF anode and therefore reduced the start-up time (Zhang et al., 2019) as shown in **Figure 2A**. Moreover, *Shinella and Comamonas* reported to have the capability to transfer electrons and decolorize azo dyes, which were present in higher abundance in PANI–SSFF–MFC (biofilm–7.4%; suspension–12%) compared to SSFF–MFC (biofilm–4.6%; suspension–2.3%) (Dhar et al., 2016; Dai et al., 2020). In the initial inoculum, suspension, and biofilm, significant differences were observed. Utilizing non-metric multidimensional scaling (NMDS) analysis, significant relationships were found among the community structure of the anodic biofilm, suspension, and the inoculum. Microbial communities sampled from biofilm and suspension of PANI-SSFF-MFC differed significantly from biofilm and suspension of SSFF-MFC due to the presence of different anodes (**Figure 7C**). In our previous work (Khan M. D et al., 2021) and the present study source of inoculum was the same. In both the studies, MFCs were run with different anodes; however, only a small change in the relative abundance of bacteria was observed, but the start-up time was different. Dye degrading and bioelectricity generating bacteria were reported to be present in SMFC treating azo dye in both studies. In addition, the inoculum community totally diverged from the biofilm and suspension community of both the SMFCs (PANI–SSFF–MFC and SSFF–MFC) and observed in a separate direction suggested that the microbial communities were well adapted to the MFC environment. According to these results, the presence of a conducting anode and an azo dye in an MFC can stimulate the growth of exoelectrogens and bacteria that degrade dyes.

CONCLUSION

The outcomes of this work revealed that an integrated PANI–SSFF–MFC–aerobic bioreactor treatment method was highly influential in succeeding in efficient biodegradation of the AB29. The PANI–SSFF–MFC offered a higher maximum power density ($103 \pm 3.6\ mW\ m^{-2}$) with correspondingly high decolorization efficiency (93 ± 3.1%) and COD removal (92.5 ± 2%). 16S rRNA sequencing analysis revealed that a large percentage of the bacterial composition in PANI–SSFF–MFC consisted of *Proteobacteria* (72%), and the majority of bacteria were designated as bioelectricity generating and/or dye degrading bacteria. The results conclude that the PANI–SSFF anode can be used to serve as a high-performance anode for the superior performance of MFC.

DATA AVAILABILITY STATEMENT

The original contributions presented in the study are publicly available. This data can be found at: https://www.ncbi.nlm.nih.gov/bioproject/, PRJNA816182.

AUTHOR CONTRIBUTIONS

MK: Conceptualization, methodology, software, data curation, investigation, writing–original draft, writing—review and editing, project administration, funding acquisition; ST: formal analysis, RT: software, formal analysis; DL: formal analysis; AA: formal analysis; KS: visualization, resources; MK: supervision, writing—review and editing, validation, project administration; EY: supervision, writing—review and editing, validation, funding acquisition, and project administration.

FUNDING

This work was supported by the Commonwealth Scholarship Commission, United Kingdom (INCN-2018-81), Natural Environment Research Council (NE/L01422X/1), and Engineering and Physical Sciences Research Council (EP/N009746/1).

ACKNOWLEDGMENTS

The authors are also grateful for the facilities provided by the School of Engineering, Newcastle University, United Kingdom, and the Aligarh Muslim University, Aligarh, as part of the research.

REFERENCES

Aiyer, K. S. (2020). How Does Electron Transfer Occur in Microbial Fuel Cells? *World J. Microbiol. Biotechnol.* 36, 1–9. doi:10.1007/s11274-020-2801-z

Al-Tohamy, R., Sun, J., Fareed, M. F., Kenawy, E.-R., and Ali, S. S. (2020). Ecofriendly Biodegradation of Reactive Black 5 by Newly Isolated Sterigmatomyces Halophilus SSA1575, Valued for Textile Azo Dye Wastewater Processing and Detoxification. *Sci. Rep.* 10, 1–16. doi:10.1038/s41598-020-69304-4

Ansari, S. A., Parveen, N., Han, T. H., Ansari, M. O., and Cho, M. H. (2016). Fibrous Polyaniline@manganese Oxide Nanocomposites as Supercapacitor Electrode Materials and Cathode Catalysts for Improved Power Production in Microbial Fuel Cells. *Phys. Chem. Chem. Phys.* 18, 9053–9060. doi:10.1039/c6cp00159a

Bhandari, S., Poudel, D. K., Marahatha, R., Dawadi, S., Khadayat, K., Phuyal, S., et al. (2021). Microbial Enzymes Used in Bioremediation. *J. Chem.* 2021, 1–17. doi:10.1155/2021/8849512

Cao, X., Zhang, S., Wang, H., and Li, X. (2019). Azo Dye as Part of Co-substrate in a Biofilm Electrode Reactor-Microbial Fuel Cell Coupled System and an Analysis of the Relevant Microorganisms. *Chemosphere* 216, 742–748. doi:10.1016/j.chemosphere.2018.10.203

Caporaso, J. G., Lauber, C. L., Walters, W. A., Berg-Lyons, D., Lozupone, C. A., Turnbaugh, P. J., et al. (2011). Global Patterns of 16S rRNA Diversity at a Depth of Millions of Sequences Per Sample. *Proc. Natl. Acad. Sci. U.S.A.* 108, 4516–4522. doi:10.1073/pnas.1000080107

Chen, B.-Y., Zhang, M.-M., Ding, Y., and Chang, C.-T. (2010). Feasibility Study of Simultaneous Bioelectricity Generation and Dye Decolorization Using Naturally Occurring Decolorizers. *J. Taiwan Inst. Chem. Eng.* 41, 682–688. doi:10.1016/j.jtice.2010.02.005

Chen, C.-Y., Tsai, T.-H., Wu, P.-S., Tsao, S.-E., Huang, Y.-S., and Chung, Y.-C. (2018). Selection of Electrogenic Bacteria for Microbial Fuel Cell in Removing Victoria Blue R from Wastewater. *J. Environ. Sci. Health A* 53, 108–115. doi:10.1080/10934529.2017.1377580

Dai, Q., Zhang, S., Liu, H., Huang, J., and Li, L. (2020). Sulfide-mediated Azo Dye Degradation and Microbial Community Analysis in a Single-Chamber Air Cathode Microbial Fuel Cell. *Bioelectrochemistry* 131, 107349. doi:10.1016/j.bioelechem.2019.107349

de Oliveira, M. A. C., Ficca, V. C. A., Gokhale, R., Santoro, C., Mecheri, B., D'Epifanio, A., et al. (2020). Iron(II) Phthalocyanine (FePc) over Carbon Support for Oxygen Reduction Reaction Electrocatalysts Operating in Alkaline Electrolyte. *J. Solid State. Electrochem.* 25, 93–104. doi:10.1007/s10008-020-04537-x

Dessie, Y., Tadesse, S., and Adimasu, Y. (2022). Improving the Performance of Graphite Anode in a Microbial Fuel Cell via PANI Encapsulated α-MnO2 Composite Modification for Efficient Power Generation and Methyl Red Removal. *Chem. Eng. J. Adv.* 10, 100283. doi:10.1016/j.ceja.2022.100283

Dhar, B. R., Ryu, H., Santo Domingo, J. W., and Lee, H.-S. (2016). Ohmic Resistance Affects Microbial Community and Electrochemical Kinetics in a Multi-Anode Microbial Electrochemical Cell. *J. Power Sourc.* 331, 315–321. doi:10.1016/j.jpowsour.2016.09.055

Fang, Z., Song, H.-l., Cang, N., and Li, X.-n. (2015). Electricity Production from Azo Dye Wastewater Using a Microbial Fuel Cell Coupled Constructed Wetland Operating under Different Operating Conditions. *Biosens. Bioelectron.* 68, 135–141. doi:10.1016/j.bios.2014.12.047

Fernando, E., Keshavarz, T., and Kyazze, G. (2014). Complete Degradation of the Azo Dye Acid Orange-7 and Bioelectricity Generation in an Integrated Microbial Fuel Cell, Aerobic Two-Stage Bioreactor System in Continuous Flow Mode at Ambient Temperature. *Bioresour. Tech.* 156, 155–162. doi:10.1016/j.biortech.2014.01.036

Fernando, E., Keshavarz, T., and Kyazze, G. (2013). Simultaneous Co-metabolic Decolourisation of Azo Dye Mixtures and Bio-Electricity Generation under Thermophillic (50°C) and saline Conditions by an Adapted Anaerobic Mixed Culture in Microbial Fuel Cells. *Bioresour. Tech.* 127, 1–8. doi:10.1016/j.biortech.2012.09.065

Fontmorin, J.-M., Hou, J., Rasul, S., and Yu, E. (2018). Stainless Steel-Based Materials for Energy Generation and Storage in Bioelectrochemical Systems Applications. *ECS Trans.* 85, 1181–1192. doi:10.1149/08513.1181ecst

Gao, Y., Ryu, H., Santo Domingo, J. W., and Lee, H.-S. (2014). Syntrophic Interactions between H2-Scavenging and Anode-Respiring Bacteria Can Improve Current Density in Microbial Electrochemical Cells. *Bioresour. Tech.* 153, 245–253. doi:10.1016/j.biortech.2013.11.077

Ge, Y., Wei, B., Wang, S., Guo, Z., and Xu, X. (2015). Optimization of Anthraquinone Dyes Decolorization Conditions with Response Surface Methodology by Aspergillus. *Korean Chem. Eng. Res.* 53, 327–332. doi:10.9713/kcer.2015.53.3.327

Gutu, L., Basitere, M., Harding, T., Ikumi, D., Njoya, M., and Gaszynski, C. (2021). Multi-Integrated Systems for Treatment of Abattoir Wastewater: A Review. *Water* 13, 2462. doi:10.3390/w13182462

Hou, J., Liu, Z., and Li, Y. (2015). Polyaniline Modified Stainless Steel Fiber Felt for High-Performance Microbial Fuel Cell Anodes. *Jocet* 3, 165–169. doi:10.7763/jocet.2015.v3.189

Khan, M. D., Abdulateif, H., Ismail, I. M., Sabir, S., and Khan, M. Z. (2015a). Bioelectricity Generation and Bioremediation of an Azo-Dye in a Microbial Fuel Cell Coupled Activated Sludge Process. *PLoS One* 10, e0138448. doi:10.1371/journal.pone.0138448

Khan, M. D., Khan, N., Sultana, S., Joshi, R., Ahmed, S., Yu, E., et al. (2017). Bioelectrochemical Conversion of Waste to Energy Using Microbial Fuel Cell Technology. *Process Biochem.* 57, 141–158. doi:10.1016/j.procbio.2017.04.001

Khan, M. D., Li, D., Tabraiz, S., Shamurad, B., Scott, K., Khan, M. Z., et al. (2021). Integrated Air Cathode Microbial Fuel Cell-Aerobic Bioreactor Set-Up for Enhanced Bioelectrodegradation of Azo Dye Acid Blue 29. *Sci. Total Environ.* 756, 0–10. doi:10.1016/j.scitotenv.2020.143752

Khan, M. Z., Singh, S., Sultana, S., Sreekrishnan, T. R., and Ahammad, S. Z. (2015b). Studies on the Biodegradation of Two Different Azo Dyes in Bioelectrochemical Systems. *New J. Chem.* 39, 5597–5604. doi:10.1039/c5nj00541h

Khan, N., Anwer, A. H., Khan, M. D., Azam, A., Ibhadon, A., and Khan, M. Z. (2021). Magnesium Ferrite Spinels as Anode Modifier for the Treatment of Congo Red and Energy Recovery in a Single Chambered Microbial Fuel Cell. *J. Hazard. Mater.* 410, 124561. doi:10.1016/j.jhazmat.2020.124561

Lai, B., Tang, X., Li, H., Du, Z., Liu, X., and Zhang, Q. (2011). Power Production Enhancement with a Polyaniline Modified Anode in Microbial Fuel Cells. *Biosens. Bioelectron.* 28, 373–377. doi:10.1016/j.bios.2011.07.050

Li, R., Li, T., Wan, Y., Zhang, X., Liu, X., Li, R., et al. (2022). Efficient Decolorization of Azo Dye Wastewater with Polyaniline/graphene Modified Anode in Microbial Electrochemical Systems. *J. Hazard. Mater.* 421, 126740. doi:10.1016/j.jhazmat.2021.126740

Liu, S., Feng, X., Gu, F., Li, X., and Wang, Y. (2017). Sequential Reduction/oxidation of Azo Dyes in a Three-Dimensional Biofilm Electrode Reactor. *Chemosphere* 186, 287–294. doi:10.1016/j.chemosphere.2017.08.001

Mehdinia, A., Dejaloud, M., and Jabbari, A. (2013). Nanostructured Polyaniline-Coated Anode for Improving Microbial Fuel Cell Power Output. *Chem. Pap.* 67, 1096–1102. doi:10.2478/s11696-013-0381-1

Obaid, A. Y., El-Mossalamy, E. H., Al-Thabaiti, S. A., El-Hallag, I. S., Hermas, A. A., and Asiri, A. M. (2014). Electrodeposition and Characterization of Polyaniline on Stainless Steel Surface via Cyclic, Convolutive Voltammetry and SEM in Aqueous Acidic Solutions. *Int. J. Electrochem. Sci.* 9, 1003–1015.

Oon, Y.-S., Ong, S.-A., Ho, L.-N., Wong, Y.-S., Oon, Y.-L., Lehl, H. K., et al. (2018). Disclosing the Synergistic Mechanisms of Azo Dye Degradation and Bioelectricity Generation in a Microbial Fuel Cell. *Chem. Eng. J.* 344, 236–245. doi:10.1016/j.cej.2018.03.060

Paquin, F., Rivnay, J., Salleo, A., Stingelin, N., and Silva-Acuña, C. (2015). Multi-phase Microstructures Drive Exciton Dissociation in Neat Semicrystalline Polymeric Semiconductors. *J. Mater. Chem. C* 3, 10715–10722. doi:10.1039/c5tc02043c

Popli, S., and Patel, U. D. (2015). Destruction of Azo Dyes by Anaerobic-Aerobic Sequential Biological Treatment: a Review. *Int. J. Environ. Sci. Technol.* 12, 405–420. doi:10.1007/s13762-014-0499-x

Quan, X., Xu, H., Sun, B., and Xiao, Z. (2018). Anode Modification with Palladium Nanoparticles Enhanced Evans Blue Removal and Power Generation in Microbial Fuel Cells. *Int. Biodeterioration Biodegradation* 132, 94–101. doi:10.1016/j.ibiod.2018.01.001

Rathour, R., Patel, D., Shaikh, S., and Desai, C. (2019). Eco-electrogenic Treatment of Dyestuff Wastewater Using Constructed Wetland-Microbial Fuel Cell System with an Evaluation of Electrode-Enriched Microbial Community Structures. *Bioresour. Tech.* 285, 121349. doi:10.1016/j.biortech.2019.121349

Rawat, D., Mishra, V., and Sharma, R. S. (2016). Detoxification of Azo Dyes in the Context of Environmental Processes. *Chemosphere* 155, 591–605. doi:10.1016/j.chemosphere.2016.04.068

Ruiz, V., Ilhan, Z. E., Kang, D.-W., Krajmalnik-Brown, R., and Buitrón, G. (2014). The Source of Inoculum Plays a Defining Role in the Development of MEC Microbial Consortia Fed with Acetic and Propionic Acid Mixtures. *J. Biotechnol.* 182-183, 11–18. doi:10.1016/j.jbiotec.2014.04.016

Shamurad, B., Gray, N., Petropoulos, E., Tabraiz, S., Acharya, K., Quintela-Baluja, M., et al. (2019). Co-digestion of Organic and mineral Wastes for Enhanced Biogas Production: Reactor Performance and Evolution of Microbial Community and Function. *Waste Manage.* 87, 313–325. doi:10.1016/j.wasman.2019.02.021

Solanki, K., Subramanian, S., and Basu, S. (2013). Microbial Fuel Cells for Azo Dye Treatment with Electricity Generation: A Review. *Bioresour. Tech.* 131, 564–571. doi:10.1016/j.biortech.2012.12.063

Sonawane, J. M., Al-Saadi, S., Singh Raman, R. K., Ghosh, P. C., and Adeloju, S. B. (2018a). Exploring the Use of Polyaniline-Modified Stainless Steel Plates as Low-Cost, High-Performance Anodes for Microbial Fuel Cells. *Electrochimica Acta* 268, 484–493. doi:10.1016/j.electacta.2018.01.163

Sonawane, J. M., Patil, S. A., Ghosh, P. C., and Adeloju, S. B. (2018b). Low-cost Stainless-Steel Wool Anodes Modified with Polyaniline and Polypyrrole for High-Performance Microbial Fuel Cells. *J. Power Sourc.* 379, 103–114. doi:10.1016/j.jpowsour.2018.01.001

Song, L., Shao, Y., Ning, S., and Tan, L. (2017). Performance of a Newly Isolated Salt-Tolerant Yeast Strain Pichia Occidentalis G1 for Degrading and Detoxifying Azo Dyes. *Bioresour. Tech.* 233, 21–29. doi:10.1016/j.biortech.2017.02.065

Sultana, S., Khan, M. D., Sabir, S., Gani, K. M., Oves, M., and Khan, M. Z. (2015). Bio-electro Degradation of Azo-Dye in a Combined Anaerobic-Aerobic Process along with Energy Recovery. *New J. Chem.* 39, 9461–9470. doi:10.1039/c5nj01610j

Sun, J., Bi, Z., Hou, B., Cao, Y.-q., and Hu, Y.-y. (2011). Further Treatment of Decolorization Liquid of Azo Dye Coupled with Increased Power Production Using Microbial Fuel Cell Equipped with an Aerobic Biocathode. *Water Res.* 45, 283–291. doi:10.1016/j.watres.2010.07.059

Sun, J., Li, Y., Hu, Y., Hou, B., Xu, Q., Zhang, Y., et al. (2012). Enlargement of Anode for Enhanced Simultaneous Azo Dye Decolorization and Power Output in Air-Cathode Microbial Fuel Cell. *Biotechnol. Lett.* 34, 2023–2029. doi:10.1007/s10529-012-1002-8

Wang, Y., Pan, Y., Zhu, T., Wang, A., Lu, Y., Lv, L., et al. (2018). Enhanced Performance and Microbial Community Analysis of Bioelectrochemical System Integrated with Bio-Contact Oxidation Reactor for Treatment of Wastewater Containing Azo Dye. *Sci. Total Environ.* 634, 616–627. doi:10.1016/j.scitotenv.2018.03.346

Xie, X., Liu, N., Yang, B., Yu, C., Zhang, Q., Zheng, X., et al. (2016). Comparison of Microbial Community in Hydrolysis Acidification Reactor Depending on Different Structure Dyes by Illumina MiSeq Sequencing. *Int. Biodeterioration Biodegradation* 111, 14–21. doi:10.1016/j.ibiod.2016.04.004

Xu, H., Wang, L., Lin, C., Zheng, J., Wen, Q., Chen, Y., et al. (2020). Improved Simultaneous Decolorization and Power Generation in a Microbial Fuel Cell with the Sponge Anode Modified by Polyaniline and Chitosan. *Appl. Biochem. Biotechnol.* 192, 698–718. doi:10.1007/s12010-020-03346-2

Xu, P., Zheng, D., Xie, Z., He, Q., and Yu, J. (2020). The Degradation of Ibuprofen in a Novel Microbial Fuel Cell with PANi@CNTs/SS Bio-Anode and CuInS2 Photocatalytic Cathode: Property, Efficiency and Mechanism. *J. Clean. Prod.* 265, 121872. doi:10.1016/j.jclepro.2020.121872

Yang, H.-Y., Liu, J., Wang, Y.-X., He, C.-S., Zhang, L.-S., Mu, Y., et al. (2019). Bioelectrochemical Decolorization of a Reactive Diazo Dye: Kinetics, Optimization with a Response Surface Methodology, and Proposed Degradation Pathway. *Bioelectrochemistry* 128, 9–16. doi:10.1016/j.bioelechem.2019.02.008

Yang, Y., Xu, M., Guo, J., and Sun, G. (2012). Bacterial Extracellular Electron Transfer in Bioelectrochemical Systems. *Process Biochem.* 47, 1707–1714. doi:10.1016/j.procbio.2012.07.032

Yaqoob, A. A., Mohamad Ibrahim, M. N., and Yaakop, A. S. (2021). Application of Oil palm Lignocellulosic Derived Material as an Efficient Anode to Boost the Toxic Metal Remediation Trend and Energy Generation through Microbial Fuel Cells. *J. Clean. Prod.* 314, 128062. doi:10.1016/j.jclepro.2021.128062

Yuan, Y., Ahmed, J., and Kim, S. (2011). Polyaniline/carbon Black Composite-Supported Iron Phthalocyanine as an Oxygen Reduction Catalyst for Microbial Fuel Cells. *J. Power Sourc.* 196, 1103–1106. doi:10.1016/j.jpowsour.2010.08.112

Zhang, P., Yang, C., Xu, Y., Li, H., Shi, W., Xie, X., et al. (2019). Accelerating the Startup of Microbial Fuel Cells by Facile Microbial Acclimation. *Bioresour. Tech. Rep.* 8, 100347. doi:10.1016/j.biteb.2019.100347

Zhong, D., Liao, X., Liu, Y., Zhong, N., and Xu, Y. (2018). Enhanced Electricity Generation Performance and Dye Wastewater Degradation of Microbial Fuel Cell by Using a Petaline NiO@ Polyaniline-Carbon Felt Anode. *Bioresour. Tech.* 258, 125–134. doi:10.1016/j.biortech.2018.01.117

Conflict of Interest: The authors declare that the research was conducted in the absence of any commercial or financial relationships that could be construed as a potential conflict of interest.

Publisher's Note: All claims expressed in this article are solely those of the authors and do not necessarily represent those of their affiliated organizations, or those of the publisher, the editors, and the reviewers. Any product that may be evaluated in this article, or any claim that may be made by its manufacturer, is not guaranteed or endorsed by the publisher.